# Biochemistry

Article

# Enhancement of RNA/Ligand Association Kinetics via an Electrostatic Anchor

Raghuvir N. Sengupta[†] and Daniel Herschlag*[,†,‡,§]

[†]Department of Biochemistry, Stanford University, Stanford, California 94305, United States
[‡]Departments of Chemical Engineering and Chemistry, Stanford University, Stanford, California 94305, United States
[§]Stanford ChEM-H (Chemistry, Engineering, and Medicine for Human Health), Stanford University, Stanford, California 94305, United States

**Ⓢ** Supporting Information
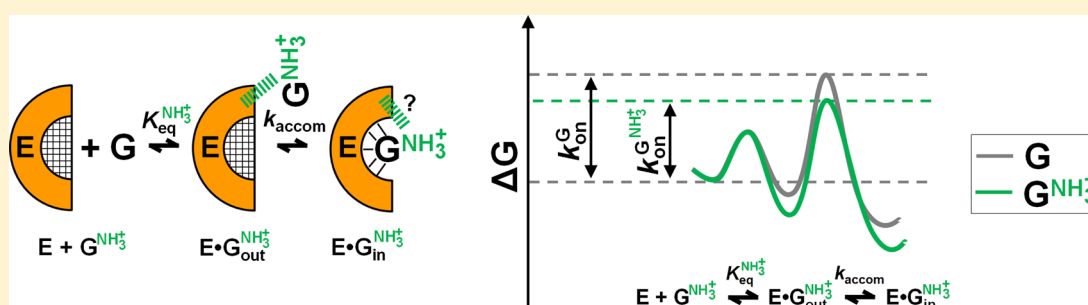
**ABSTRACT:** The diverse biological processes mediated by RNA rest upon its recognition of various ligands, including small molecules and nucleic acids. Nevertheless, a recent literature survey suggests that RNA molecular recognition of these ligands is slow, with association rate constants orders of magnitude below the diffusional limit. Thus, we were prompted to consider strategies for increasing RNA association kinetics. Proteins can accelerate ligand association via electrostatic forces, and here, using the *Tetrahymena* group I ribozyme, we provide evidence that electrostatic forces can accelerate RNA/ligand association. This RNA enzyme (E) catalyzes cleavage of an oligonucleotide substrate (S) by an exogenous guanosine (G) cofactor. The G 2′- and 3′-OH groups interact with an active site metal ion, termed $M_C$, within E·S·G, and we perturbed each of these contacts via $-NH_3^+$ substitution. New and prior data indicate that $G(2'NH_3^+)$ and $G(3'NH_3^+)$ bind as strongly as G, suggesting that the $-NH_3^+$ substituents of these analogues avoid repulsive interactions with $M_C$ and make alternative interactions. Unexpectedly, removal of the adjacent $-OH$ via $-H$ substitution to give $G(2'H,3'NH_3^+)$ and $G(2'NH_3^+,3'H)$ enhanced binding, in stark contrast to the deleterious effect of these substitutions on G binding. Pulse−chase experiments indicate that the $-NH_3^+$ moiety of $G(2'H,3'NH_3^+)$ increases the rate of G association. These results suggest that the positively charged $-NH_3^+$ group can act as a molecular "anchor" to increase the residence time of the encounter complex and thereby enhance productive binding. Electrostatic anchors may provide a broadly applicable strategy for the development of fast binding RNA ligands and RNA-targeted therapeutics.

Molecular recognition is critical for the function of RNAs and RNA−protein complexes that carry out biological function and regulation. RNA molecular recognition is exemplified in riboswitches, which are prevalent in prokaryotes and recognize a wide range of small molecule ligands,[1−3] in aptamers obtained by *in vitro* selection,[4−6] and in the recognition of guanosine to stimulate group I intron self-splicing.[7,8] The role of RNA in biology was presumably more widespread early in evolution, prior to the emergence of proteins,[9−11] and there may be additional yet unrecognized extant biological roles of small molecule RNA recognition.

Recently, we compiled literature RNA/ligand association data and found uniformly slow association rate constants relative to diffusion and relative to the rates observed for proteins binding to their ligands.[12] This observation may reflect the basic physical properties of RNA[12−15] and may have

limited the cellular processes selected by Nature to operate or be controlled by RNA in modern-day biology. Given the fundamental importance of RNA/ligand associations in current biology and in evolution,[12] the re-emergence of interest in RNA as a potential drug target,[16−18] and the potential to utilize RNA in synthetic biology,[19] understanding molecular recognition by RNA and how its association kinetics might be enhanced is important.

Electrostatic forces are widespread in biology and are often critical for fast and strong binding. For proteins, such forces are important in the recognition of charged ligands[20−24] and, with respect to association rates, local protein electrostatic fields can

attract oppositely charged ligands to provide binding rate constants at and in excess of the diffusion "limit".[25−30] Electrostatic fields are also presumably critical for enabling one-dimensional diffusion of proteins along DNA and thus efficient searches for specific recognition sequences and damaged DNA bases.[31−33]

For RNA, the negative charge on its phosphodiester backbone creates a powerful electrostatic potential for binding to cationic ligands. These electrostatics are most broadly manifest in the ion atmosphere that surrounds RNA molecules,[34−36] a preponderance of cations that contribute to overall neutralization as predicted for polyelectrolytes such as RNA and DNA from simple electrostatic theories.[34,35,37,38] Beyond the general attraction of positively charged ions, RNA often binds tightly to cationic small molecules, including polyamines and aminoglycoside antibiotics (e.g., refs 39−44), as well as peptide sequences rich in acidic residues (e.g., lysine and arginine),[45−48] with affinities in the micromolar and sub-micromolar range. Many of these charged ligands bind to several RNAs, and such broad specificity may reflect RNA's inherent tendency to assume stable alternative structures[14,15] that can make favorable electrostatic contacts with cationic ligands.

In the course of exploring a paradoxical observation for molecular recognition by the *Tetrahymena* group I ribozyme, we uncovered an electrostatic enhancement of RNA/ligand association. As described below, our results led to a recognition model via an electrostatic "binding anchor" to increase the efficiency and rate of binding. This approach may be of value in the design of RNA ligands in engineering and therapeutics.

## ■ MATERIALS AND METHODS

**Materials.** L-21 *Sca*I ribozyme (E) was transcribed and gel-purified according to reported procedures.[49] Care was taken to avoid RNA damage from ultraviolet shadowing, as previously described.[50] Guanosine (G) was purchased from Sigma-Aldrich (St. Louis, MO) with a purity of ≥98%, and 3′-aminoguanosine [G(2′N)] and 3′-amino-2′-deoxyguanosine [G(2′H,3′N)] were purchased from Santa Cruz Biotechnology (Santa Cruz, CA) and were of the highest purity commercially available (≥98%). 2′-Amino-3′-deoxyguanosine [G(2′N,3′H)] was a gift from J. W. Szostak (Harvard University, Cambridge, MA). The oligonucleotide substrates, CCCUCUA (rSA) and CCCUCdUA (−1d,rSA), were purchased from Integrated DNA Technologies (Redwood City, CA), 5′-$^{32}$P-radiolebeled using [$\gamma$-$^{32}$P]ATP (MP Biomedicals, Santa Ana, CA) and T4 polynucleotide kinase (New England Biolabs, Ipswich, MA) according to the manufacturer's protocol, and gel-purified as previously described.[51] Buffers and salts were purchased from Sigma-Aldrich. All nonradioactive reagents were passed through a 0.2 $\mu$m sterile syringe filter (Corning, Corning, NY) prior to use.

**General Reaction Conditions.** Single-turnover reactions, with ribozyme in excess of radiolabeled substrate, were measured at 30 °C in the presence of MgCl₂ (10−100 mM) and 50 mM buffer. The following buffers were used in ribozyme-catalyzed reactions: sodium acetate, pH 5.0−5.5; NaMES, pH 6.1−6.7; NaMOPS, pH 7.1; NaEPPS, pH 7.7−8.2; and NaCHES, pH 8.7−9.7.

Reactions were carried out and analyzed according to reported procedures.[7] Ribozyme was allowed to fold in 10 mM MgCl₂ and 50 mM buffer at 50 °C for 30 min and then cooled to room temperature. For reactions above pH 8.0, the folding

step was performed in 25 mM NaMES (pH 6.7) to avoid ribozyme degradation. Following the folding step, ribozyme was diluted 20-fold in reaction tubes containing the desired concentrations of divalent metal ion (MgCl₂ and MnCl₂), buffer, and G/G analogue. After a 5 min incubation at 30 °C, reactions were initiated by the addition of a labeled substrate (<0.1 nM). At specified times, six 2 $\mu$L aliquots of the reaction mixture were removed from the 20 $\mu$L reaction mixture and added to a 4 $\mu$L quench solution containing 90% formamide, 50 mM EDTA, 0.01% bromophenol blue, and 0.01% xylene cyanol. The substrate and product were separated by electrophoresis on a 20% polyacrylamide gel containing 7 M urea, 100 mM Tris, 83 mM boric acid, and 1 mM EDTA. The ratio of substrate to product was quantitated through phosphorimager analysis (GE Healthcare) with TotalLab (TotalLab Ltd.).

Reactions were followed for ≥3$t_{1/2}$ except for very slow reactions. First-order fits ($R^2 > 0.95$) to the data points, with end points of ≥90%, were obtained (KaleidaGraph, Synergy Software). The slow reactions were typically linear for up to 20 h, and an end point of 95% was assumed to obtain observed rate constants from the initial rates.

**Measurement of Affinities of G for E·S.** The binding affinity of G for the E·S complex was determined by measuring the observed rate of cleavage ($k_{obs}$) of 5′-end-labeled rSA (or −1d,rSA) at different G concentrations under conditions where E is saturating with respect to S ([E] = 50 nM; $K_d^S \sim 1$ nM).[52] $k_{obs}$ was plotted as a function of G concentration, and the data were fit to eq 1 to obtain $K_{1/2}^G$.

$$k_{obs} = \frac{k_{max}[G]}{[G] + K_{1/2}^G} \tag{1}$$

To ensure that $K_{1/2}^G$ is equal to $K_d^G$, we used the rSA substrate at pH <6 as prior data indicate that the chemical step is rate-limiting at and below this pH.[53−55] Above pH 6, we used the −1d,rSA substrate that contains a 2′-H substitution at the U(−1) position that renders the chemical step rate-limiting.[53−55]

**Measurement of Affinities of G(3′N), G(2′H,3′N), and G(2′N,3′H) for E·S.** We did not observe any detectable cleavage activity for G(3′N), G(2′H,3′N), and G(2′N,3′H) and thus measured binding of these analogues to E·S through competitive inhibition of the reaction E·S + G → products. Experiments were performed using 5′-end-labeled rSA (or −1d,rSA) with E saturating with respect to S (see above) and with subsaturating G ([G] = 30 $\mu$M; $K_d^G \sim 100$ $\mu$M).[53] The concentration of inhibitor, G$_X$, was varied, and the inhibition constant, $K_i$, that reports the affinity of G$_X$ for E·S was determined via eq 2:

$$k_{obs} = \frac{k_{max}K_i}{K_i + [G_X]} \tag{2}$$

where $k_{obs}$ is the observed rate of cleavage of rSA (or −1d,rSA) and $k_{max}$ is $k_{obs}$ in the absence of an inhibitor.

**Monitoring Binding of G(3′NH₃⁺), G(2′H,3′NH₃⁺), and G(2′NH₃⁺,3′H) to E·S.** The −NH₂ groups of G(3′N), G(2′H,3′N), and G(2′N,3′H) can ionize to form the corresponding −NH₃⁺ species. To ensure that we were monitoring the −NH₃⁺ forms of these analogues, we measured the binding of each analogue at various pH values (Figures S1−S3). For all guanosine analogues bearing the −NH₂ moiety, we observed that the level of binding to E·S increased

with a decrease in pH and did not vary below pH 6. The data were fit to an equation for binding of the $-NH_2$ and $-NH_3^+$ forms of $G(3'N)$, $G(2'H,3'N)$, and $G(2'N,3'H)$ (Figures S1–S3) to obtain binding constants for the neutral and protonated forms of these analogues.

**Pulse–Chase Assay for Measuring $k_{off}$ for G-$(2'H,3'NH_3^+)$.** To measure the dissociation rate constant $(k_{off})$ for $G(2'H,3'NH_3^+)$, we carried out a pulse−chase assay. In a typical experiment, 5′-end-labeled rSA ($[*S] < 1$ nM) was incubated with saturating ribozyme ($[E] = 100$ nM; $K_d^S \sim 1$ nM) and saturating $G(2'H,3'NH_3^+)$ $\{[G(2'H,3'N)] = 350$ nM; $K_d^{G(2'H,3'NH_3^+)} = 94$ nM (Table S2)$\}$ at various times ($t_1 = 1$, 10, and 60 min) in 50 mM sodium acetate (pH 5.5) and 10 mM $Mg^{2+}$. After $t_1$, the reaction mixture was diluted 10-fold with a chase solution containing 2 mM G, 50 mM sodium acetate (pH 5.5), and 10 mM $Mg^{2+}$. Following addition of the chase, six 2 μL aliquots were withdrawn at various times ($t_2$) and added to a 4 μL quench solution containing 90% formamide, 50 mM EDTA, 0.01% bromophenol blue, and 0.01% xylene cyanol. The substrate and product were separated and analyzed as described above.

## ■ RESULTS

The *Tetrahymena* group I ribozyme (E) catalyzes cleavage of an oligonucleotide substrate (S) by an exogenous guanosine (G) cofactor. We previously provided biochemical evidence for metal ion interactions between the G 2′- and 3′-OH groups and an active site metal ion termed $M_C$ (Figure 1) through assays that replaced each of these −OH groups with an amino $(-NH_2)$ moiety,[7,56] and these interactions are consistent with X-ray crystallographic models.[57,58] Below we describe the surprising effects of the protonated $(-NH_3^+)$ forms of these analogues, $G(2'NH_3^+)$ and $G(3'NH_3^+)$, on binding to the *Tetrahymena* ribozyme.

Despite the proximity of the G 2′- and 3′-OH groups to an active site $Mg^{2+}$ ion $[M_C$ (Figure 1)], prior work showed that replacing the G 2′-OH group with an $-NH_3^+$ moiety $[G(2'NH_3^+)$ (Table 1)] does not weaken its binding to the E·S complex.[59] This observation is consistent with a model in which the positively charged $2'-NH_3^+$ group of $G(2'NH_3^+)$ interacts with one or more negatively charged phosphoryl groups near the G 2′-moiety. The affinity of $G(2'NH_3^+)$ is weakened with an increase in the concentration of the divalent metal ion $(Mg^{2+}$ and $Mn^{2+})$, and the $Mn^{2+}$ concentration dependence of this weakening suggests that $M_C$ is responsible for this effect, perhaps via electrostatic repulsion with the $2'-NH_3^+$ group or by directly competing with $G(2'NH_3^+)$ for an interaction with one or more active site phosphoryl groups (Figure 1B).[59] To learn more about potential electrostatic interactions in and around this site, we carried out analogous experiments with a 3′-G analogue in which the 3′-OH is replaced with an $-NH_3^+$ $[G(3'NH_3^+)$ (Table 1)].

Equilibrium constants for binding of $G(3'NH_3^+)$ to E·S were obtained by measuring binding of 3′-aminoguanosine through competitive inhibition of reactions with subsaturating G under single-turnover conditions so that the observed inhibition constant is equivalent to the dissociation constant. We measured binding of the analogue across a pH range to ensure that we were measuring binding of $G(3'NH_3^+)$ and not $G(3'NH_2)$. As expected, decreasing the pH altered the 3′-aminoguanosine affinity but did not change G binding (Figures S1 and S4). The $G(3'NH_3^+)$ data were fit to a model for
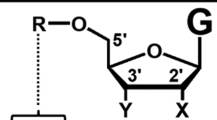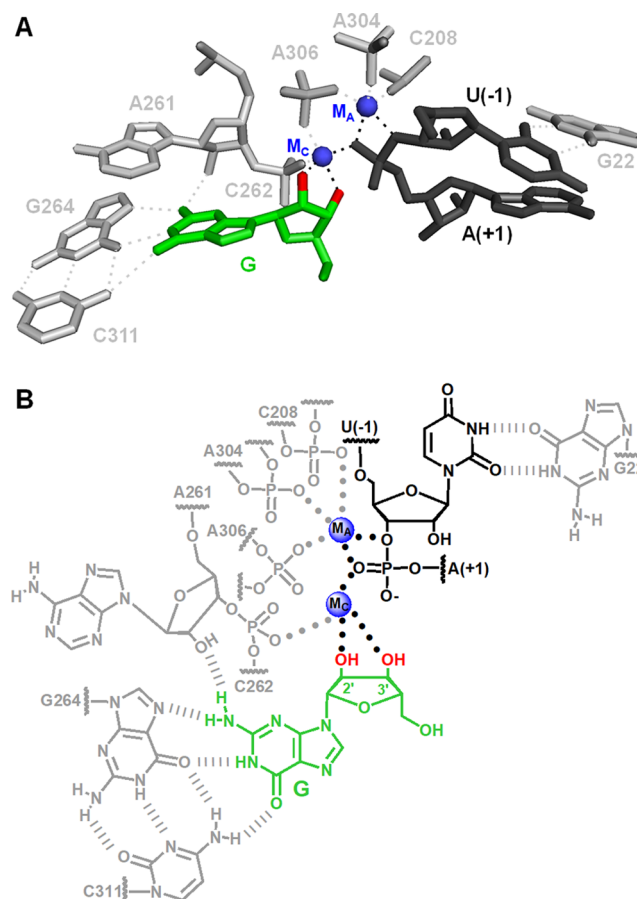


**Figure 1.** Model of active site interactions in the E·S·G complex of the *Tetrahymena* ribozyme. (A) Atomic model of interactions made with G (green) and S (black) by E (gray). Dotted lines correspond to metal ion or hydrogen bond interactions. Contacts made between $M_A$ and $M_C$ (blue) and G and S are colored black, while all other interactions are colored gray. The G 2′- and 3′-OH groups, which are modified in this work, are colored red. The model was obtained through molecular modeling of an X-ray structure of the *Azoarcus* group I ribozyme using constraints from available functional data as described previously (ref 7 and references therein). (B) Schematic of active site interactions shown in panel A, with filled circles and hatched lines representing metal ion and hydrogen bond interactions, respectively.

binding of the $-NH_3^+$ and $-NH_2$ forms of 3′-aminoguanosine to obtain the $G(3'NH_3^+)$ affinity.

Equilibrium binding constants for G and $G(3'NH_3^+)$ are listed in Table 2, and for comparison, we include the previously reported data for $G(2'NH_3^+)$[59] as well as data for G analogues with −H substitutions at the 2′- or 3′-positions.[7] The relative effects of −H and $-NH_3^+$ substitutions on G binding are presented graphically in Figure 2. Deoxy substitution at the 2′- or 3′-positions weakens binding of G by 60- or 260-fold, respectively, consistent with a model in which these −OH groups contact $M_C$ in the E·S·G complex[7,56−58] and the G 2′-OH serves as a hydrogen bond donor.[60] While substantially weaker binding of $G(2'NH_3^+)$ and $G(3'NH_3^+)$ is predicted from the close juxtaposition of the G 2′- and 3′-moieties to $M_C$, respectively, both analogues bind 2-fold stronger than G (Figure 2). These results are consistent with a model in which the $3'-NH_3^+$ group of $G(3'NH_3^+)$ makes a favorable interaction with one or more active site residues, analogous to prior observations with $G(2'NH_3^+)$.[59]

**Table 1. Guanosine (G) Analogues Used in This Work**[a]

| Abbreviation | R−O | Y | X |
|---|---|---|---|
| G | H | OH | OH |
| G(2′NH$_3^+$) | H | OH | NH$_3^+$ |
| G(3′NH$_3^+$) | H | NH$_3^+$ | OH |
| G(2′NH$_3^+$, 3′H) | H | H | NH$_3^+$ |
| G(2′H, 3′NH$_3^+$) | H | NH$_3^+$ | H |
| AUCG | AUC | OH | OH |
| AUCG(2′H) | AUC | OH | H |
| AUCG(3′H) | AUC | H | OH |

[a]The 5′-AUC extension enhances binding of the 3′-terminal G residue via base pairing and stacking interactions (forming P9.0 with the ribozyme) and overcoming assay limitations caused by the limited solubility of G(2′H) and G(3′H) (see ref 7 and references therein).

**Table 2. Effects of Deoxy (−H) and Protonated Amino (−NH$_3^+$) Substitutions on Binding of G to E·S**[a]

| G Analog | $K_d$ (μM) | 1/$K_d^{rel}$ |
|---|---|---|
| G | 127 ± 40 | (1.0) |
| G(2′NH$_3^+$) | 63 | 2.0 |
| G(2′NH$_3^+$,3′H) | 11 ± 0.5 | 11.5 |
| G(3′NH$_3^+$) | 52 ± 5 | 2.4 |
| G(2′H,3′NH$_3^+$) | 0.27 ± 0.01 | 470 |
| AUCG | 0.32 ± 0.05 | (1.0) |
| AUCG(2′H) | 20 ± 3 | 0.016 |
| AUCG(3′H) | 82 ± 11 | 0.0039 |

[a]$K_d^{rel} = K_d^{G\ analogue}/K_d^G$. $K_d$s for G, G(2′NH$_3^+$,3′H), G(3′NH$_3^+$), and G(2′H,3′NH$_3^+$) are from Figures S1−S4 and were measured in the presence of 100 mM Mg$^{2+}$. G(2′NH$_3^+$) data were from ref 59 and measured in the presence of 100 mM Mg$^{2+}$. AUCG data were from ref 7 and measured in the presence of 50 mM Mg$^{2+}$.
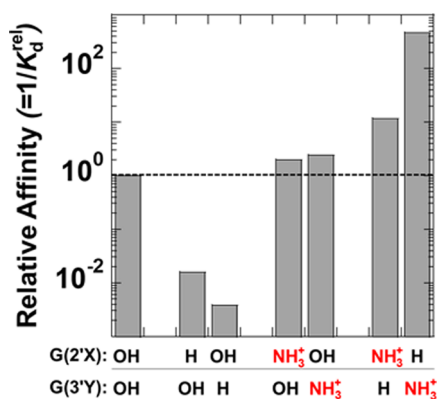


**Figure 2.** Binding of G and G analogues to E·S. The relative affinity (=1/$K_d^{rel}$ = $K_d^{G\ analogue}/K_d^G$) refers to the $K_d$ for the G or AUCG analogue relative to G or AUCG. Values of $K_d^{rel}$ were obtained from Table 2. The dashed line corresponds to $K_d^{rel} = 1$.

Having observed that G(2′NH$_3^+$) and G(3′NH$_3^+$) form stable complexes with the ribozyme, we next asked whether M$_C$ competes with G(3′NH$_3^+$) for binding to the ribozyme, as inferred for G(2′NH$_3^+$).[59] We therefore measured binding of G(3′NH$_3^+$) at various Mg$^{2+}$ and Mn$^{2+}$ concentrations (Figures S5 and S6). Surprisingly, increasing the concentration of Mg$^{2+}$

from 2 to 100 mM weakened binding of G(3′NH$_3^+$) by only 4-fold (Figure S5), in contrast to the 60-fold decrease in the level of binding observed for G(2′NH$_3^+$).[59] Furthermore, binding of G(3′NH$_3^+$) was unaffected by the addition of Mn$^{2+}$ (Figure S5), whereas Mn$^{2+}$ destabilizes G(2′NH$_3^+$) binding by at least a 100-fold.[59] The observation that Mg$^{2+}$ and Mn$^{2+}$ have no or little effect on binding of G(3′NH$_3^+$) (Table S1) is consistent with a model in which this G analogue is bound in an alternative configuration, with the 3′-NH$_3^+$ positioned away from M$_C$. Thus, although the adjacent G 2′- and 3′-OH groups both contact M$_C$ (Figure 1), replacing either −OH with an −NH$_3^+$ modification leads to different outcomes in how these G analogues are bound within the active site.

To test the model described above and potentially learn more about these alternative binding modes, we determined the effects of removing the adjacent −OH group of G(2′NH$_3^+$) and G(3′NH$_3^+$) on binding to the ribozyme. If the interaction between M$_C$ and the G 2′-OH group of G(3′NH$_3^+$) [or the G 3′-OH group of G(2′NH$_3^+$)] were retained, ablating the −OH moiety via −H substitution is, most simply, expected to destabilize binding. Alternatively, if these analogues can access alternative binding modes via the −NH$_3^+$ substituent, the affinities of the analogues could remain the same or even increase. We therefore measured binding of protonated 3′-deoxy-2′-aminoguanosine and 2′-deoxy-3′-aminoguanosine [G(2′NH$_3^+$,3′H) and G(2′H,3′NH$_3^+$), respectively (Table 1)], following procedures analogous to those described above for G(3′NH$_3^+$) (see Figures S2 and S3).

The relative effects of −H and −NH$_3^+$ substitutions on G binding to E·S are summarized in Figure 2. Whereas replacing the 2′- and 3′-OH groups with −H weakens binding of G, removal of the neighboring OH groups strengthens binding of G(2′NH$_3^+$) and G(3′NH$_3^+$), with G(2′NH$_3^+$,3′H) and G(2′H,3′NH$_3^+$) binding ∼10- and 470-fold stronger than G, respectively (Figure 2). In addition, Mg$^{2+}$ and Mn$^{2+}$ had little effect on binding of G(2′H,3′NH$_3^+$) (Table S2), suggesting that M$_C$ does not compete with this analogue for binding to the ribozyme. These results support binding in alternative modes within the active site of the *Tetrahymena* ribozyme, and the 1−3 kcal/mol strengthened binding presumably reflects new, fortuitous interactions made with the ammonium groups of G(2′NH$_3^+$) and G(3′NH$_3^+$) that are easier to access without steric restrictions to ribose ring motion and/or steric hindrance by the neighboring OH groups.

We considered two initial classes of models for the unexpected tight binding of G(2′H,3′NH$_3^+$) to E·S. (I) Major active site reorganization is required for G(2′H,3′NH$_3^+$) binding; this process would most simply be expected to slow binding by presenting an additional step and energetic barrier but decrease $k_{off}$ because of the additional strong electrostatic interaction. (II) A strong electrostatic interaction tethers the G analogue as a first step in the binding process, increasing the binding rate by providing time for rearrangement to a binding competent active site conformation. As these models are not mutually exclusive, both factors could be in play. To evaluate these models, we probed $k_{off}$ and $k_{on}$ for G(2′H,3′NH$_3^+$).

To measure $k_{off}$ for G(2′H,3′NH$_3^+$), we utilized a pulse−chase assay, which involves incubating the ribozyme with radiolabeled S and G(2′H,3′NH$_3^+$) at various times to form the E·S·G(2′H,3′NH$_3^+$) complex (Figure 3A). We subsequently diluted the sample 10-fold in a chase solution containing excess G to prevent rebinding of G(2′H,3′NH$_3^+$) that had dissociated from the ribozyme before or after addition
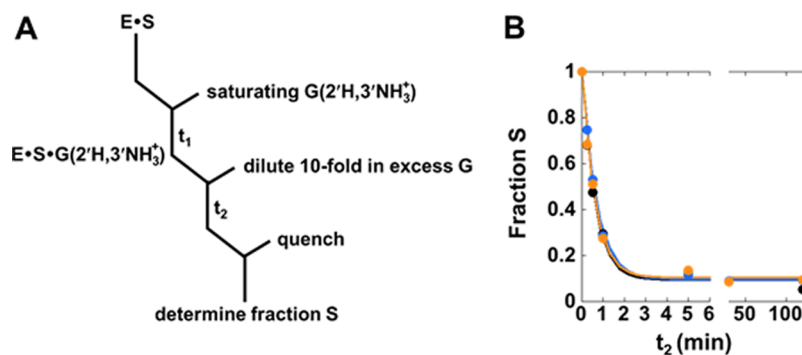
**Figure 3.** Pulse—chase assay for measuring $k_{off}$ for G(2′H,3′NH$_3^+$). (A) Scheme for the pulse—chase assay. (B) Plot of the fraction of S vs $t_2$ at $t_1 =$ 1 min (black circles), 10 min (blue circles), and 60 min (orange circles). The lines are first-order fits of the data, giving rate constants of 1.6, 1.5, and 1.6 min$^{-1}$ at $t_1$ values of 1, 10, and 60 min, respectively. Pulse—chase experiments were performed with the rSA substrate at pH 5.5 in the presence of 10 mM Mg$^{2+}$ at 30 °C, as described in Materials and Methods.

**Table 3. Binding of G and G(2′H,3′NH$_3^+$) to E·S$^a$**

| G analogue | $K_d$ ($\mu$M) | $1/K_d^{rel}$ | $k_{off}$ (min$^{-1}$) | $1/k_{off}^{rel}$ | $k_{on}$ (M$^{-1}$ min$^{-1}$) | $k_{on}^{rel}$ |
|---|---|---|---|---|---|---|
| G | 110 | (1.0) | 44 | (1.0) | $4.0 \times 10^5$ | (1.0) |
| G(2′H,3′NH$_3^+$) | 0.094 | 1170 | >2 | <22 | >2.1 × 10$^7$ | >53 |

$^a K_d$ and $k_{on}$ values for G obtained from ref 61. $k_{off}$ was calculated from the equation $k_{off} = K_d k_{on}$. $K_d$ and $k_{off}$ values for G(2′H,3′NH$_3^+$) obtained from Table S2 and Figure 3, respectively, and $k_{on}$ was calculated from the equation $k_{on} = k_{off}/K_d$. $K_d^{rel} = K_d^{G\ analogue}/K_d^G$. $k_{off}^{rel} = k_{off}^{G\ analogue}/k_{off}^G$. $k_{on}^{rel} = k_{on}^{G\ analogue}/k_{on}^G$. All data were measured in the presence of 10 mM Mg$^{2+}$.

of the chase. Under the conditions of our experiment, binding of G to E·S leads to rapid cleavage of S from the E·S·G complex with a rate constant of approximately 2 min$^{-1}$,[53] providing us with a readout for monitoring changes in the fraction of E·S with G(2′H,3′NH$_3^+$) bound.

If the dissociation rate constant ($k_{off}$) for G(2′H,3′NH$_3^+$) is smaller than the rate of cleavage of S from the E·S·G complex (i.e., $k_{off}$ < 2 min$^{-1}$), cleavage of S following addition of the chase solution is expected to be biphasic, with a fast phase corresponding to the fraction of ribozyme without G-(2′H,3′NH$_3^+$) bound and a slow phase corresponding to dissociation of G(2′H,3′NH$_3^+$) from the E·S·G(2′H,3′NH$_3^+$) complex that allows formation of the productive E·S·G complex. In contrast, if the G(2′H,3′NH$_3^+$) rate of dissociation exceeds that for cleavage of S from E·S·G (i.e., $k_{off}$ > 2 min$^{-1}$), cleavage of S is expected to be monophasic following addition of the chase, with a rate constant of 2 min$^{-1}$.

As shown in Figure 3B, we observed monophasic kinetics with a rate constant of ~2 min$^{-1}$ for cleavage of S in our pulse—chase experiments. This value, which is identical to the rate constant for cleavage of S from the E·S·G complex, indicates that $k_{off}$ is considerably greater than 2 min$^{-1}$ for G(2′H,3′NH$_3^+$). From the conservative limit for $k_{off}$ of >2 min$^{-1}$ and the observed $K_d$ of 94 nM (Table S2), a lower limit for $k_{on}$ (=$k_{off}/K_d$) of 2.1 × 10$^7$ M$^{-1}$ min$^{-1}$ is obtained (Table 3). This limit is 53-fold higher than the rate constant for G binding of 4 × 10$^5$ M$^{-1}$ min$^{-1}$ obtained previously,[61] indicating that at least 53-fold of the overall 1170-fold stronger affinity of G(2′H,3′NH$_3^+$) versus that of G arises from an increase in $k_{on}$ and at most 22-fold of the enhanced binding arises from a decrease in $k_{off}$ (Table 3).$^a$

## ■ DISCUSSION

RNA recognition of ligands is orders of magnitude slower than diffusion, indicating that most RNA/ligand collisions are not productive; i.e., they do not lead to formation of the stable bound complex.[12] As this slow binding is observed for all

natural and *in vitro*-selected RNAs studied to date, slow recognition may be a general property of RNA and thus a property that may have affected function in an RNA world, the transition to the modern-day protein world, and the ability to efficiently engineer RNA/ligand interaction and target RNA with drugs.[12] Several potential mechanisms could be responsible for RNA's slow binding,[12] and there is support from both structural and functional studies for the simplest of these models, required conformational rearrangements between the free RNA and the bound state that are unfavorable and slow (e.g., refs 61−64).

The fastest binding to RNA (other than by proteins, where RNA can be considered the ligand[12]) is duplex formation (Figure 4).[65−67] There, an initial unstable complex forms, presumably with a single base pair, that can either dissociate
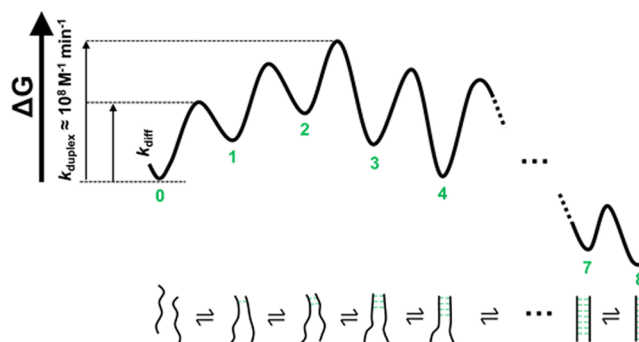


**Figure 4.** Free energy diagram for simple duplex formation according to a zipper model. A diffusion-limited encounter ($k_{diff}$) leads to formation of an unstable complex consisting of a single base pair that can dissociate or form additional base pairs. After 2−3 base pairs form, subsequent base pair formation is favored over dissociation of the complex. The rate of association between the two strands of RNA is limited by the nucleation rate for forming 2−3 base pairs ($k_{duplex}$ ~ 10$^8$ M$^{-1}$ min$^{-1}$). Adapted from ref 12.
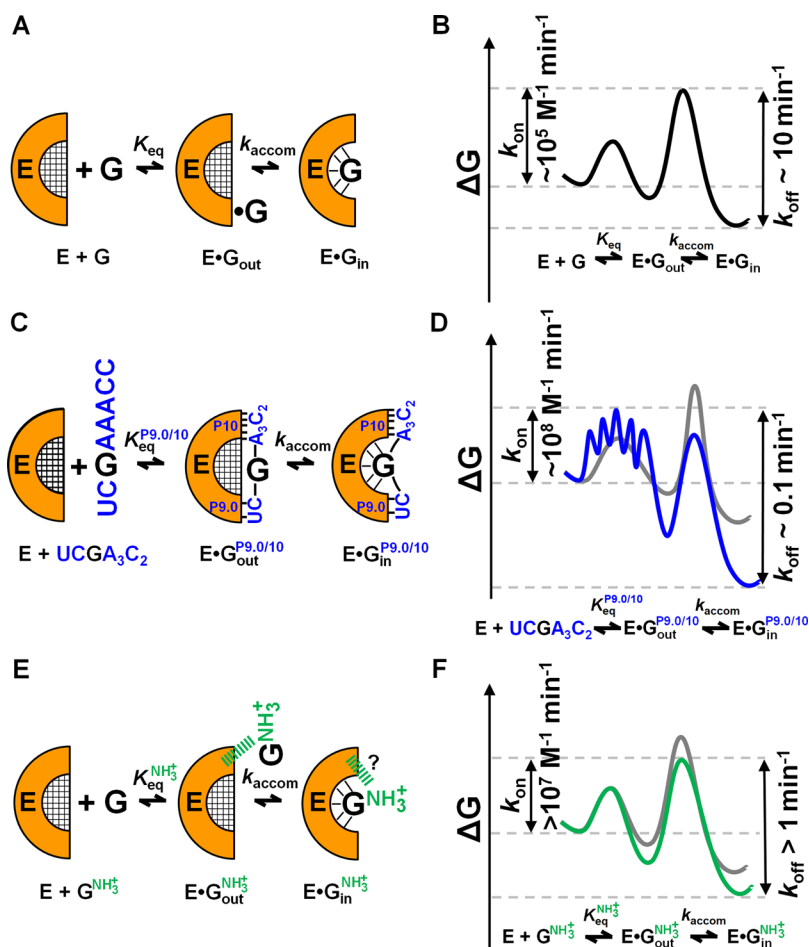
**Figure 5.** Free energy diagrams for effects of binding substeps on association and dissociation kinetics for G and G analogues with the *Tetrahymena* ribozyme. (A) Model and (B) free energy diagram for binding of G. A diffusion-limited step leads to formation of a weak complex between G and the ribozyme (E·$G_{out}$). The G binding site on the ribozyme must then undergo a conformational rearrangement to accommodate G ($k_{accom}$) to form E·$G_{in}$. Prior data (ref 61) indicate that the rate of this step is slow ($k_{accom} \sim 10^4$ min$^{-1}$) such that most G molecules dissociate instead of binding to the G binding site, and the observed association rate constant for G ($k_{on} \sim 10^5$ M$^{-1}$ min$^{-1}$) is orders of magnitude below the rate of diffusion. The calculated equilibrium constant for formation of E·$G_{out}$ [$K_{eq} = k_{on}/k_{accom} = (10^5$ M$^{-1}$ min$^{-1})/(10^4$ min$^{-1})$] is 10 M$^{-1}$, suggesting that the initial binding step involves some weak stabilizing interactions. (C) Model and (D) free energy diagram for binding of UCGAAACC. Residues 5′ and 3′ to G (UC and AAACC, respectively) base pair with the ribozyme, forming the P9.0 and P10 helices, respectively (E·$G_{out}^{P9.0/10}$). Rearrangement of the G binding site enables accommodation of G, forming E·$G_{in}^{P9.0/10}$. The free energy diagram for this process is shown in panel D (blue line), and for comparison, we show the profile for G from panel B (gray line). Prior data (ref 61) indicate the P9.0 and P10 helices increase the residence time of E·$G_{out}^{P9.0/10}$ such that the rate of association for UCGAAACC ($k_{on}$) is ~$10^8$ M$^{-1}$ min$^{-1}$, similar to rate constants for duplex formation. From a $k_{accom}$ of ~$10^4$ min$^{-1}$, the equilibrium constant for formation of E·$G_{out}^{P9.0/10}$ ($K_{eq}^{P9.0/10}$) is calculated to be $10^4$ M$^{-1}$ [$=k_{on}/k_{accom} = (10^8$ M$^{-1}$ min$^{-1})/(10^4$ min$^{-1})$]. (E) Model and (F) free energy diagram for binding of G(2′H,3′$NH_3^+$). The positively charged amino group of G(2′H,3′$NH_3^+$) (colored green; the 2′-H substituent is not shown for the sake of simplicity) forms favorable interactions with the ribozyme (denoted by hatched lines) within E·$G_{out}^{NH_3^+}$. This "binding anchor" increases the residence time of E·$G_{out}^{NH_3^+}$ for subsequent accommodation of the G analogue. The interaction made with the $NH_3^+$ substituent in E·$G_{out}^{NH_3^+}$ may or may not be retained within E·$G_{in}^{NH_3^+}$, and this is denoted by a question mark in panel E. The free energy diagram for this process is shown in panel F (green line), and for comparison, we show the profile for G from panel B (gray line). The data from Table 3 suggest that the −$NH_3^+$ substituent on G(2′H,3′$NH_3^+$) stabilizes E·$G_{out}^{NH_3^+}$ so that $k_{on}$ is >$10^7$ M$^{-1}$ min$^{-1}$. From a $k_{accom}$ of ~$10^4$ min$^{-1}$, the equilibrium constant for formation of E·$G_{out}^{NH_3^+}$ ($K_{eq}^{NH_3^+}$) is calculated to be >$10^3$ M$^{-1}$ ($=k_{on}/k_{accom}$).

(nonproductive binding) or allow formation of a second and then third base pair, etc., to give stable complex formation. While dissociation of the single-base pair complex is more likely than formation of the next pair, its hydrogen bonds cause it to persist longer than a simple encounter complex that lacks stabilizing interactions, thereby making formation of the second interaction (in this case another base pair) more likely than it would otherwise be.

Thus, interactions that can increase the lifetime of an early binding complex can increase the efficiency and rate of

binding. Such a mechanism was found for guanosine (G) recognition by the *Tetrahymena* group I intron and may play a role in the specificity of self-splicing[61] (Figure 5A,B). Pre-steady-state kinetic studies revealed a "gating" step in G binding to the *Tetrahymena* ribozyme with an estimated rate constant of ~$10^4$ min$^{-1}$, such that most G molecules would dissociate before this "binding gate" would open, resulting in the slow observed binding with a rate constant of ~$10^5$ M$^{-1}$ min$^{-1}$ (Figure 5A,B). Adding residues 5′ and/or 3′ to the G that can form base pairs (Figure 4) adjacent to the G site

results in longer residence times and more efficient (faster) binding (Figure 5C,D). When these residence times become longer than the gating time (i.e., longer than $\sim 1/10^4$ min$^{-1}$ or $\sim 10$ ms), then G, in its oligonucleotide form, can bind as fast as the upstream or downstream helix forms, with a rate constant of $\sim 10^8$ M$^{-1}$ min$^{-1}$ as is typical for RNA duplex formation (Figure 5C,D).

Our observed faster binding of a G analogue with a positively charged amino group appears to be another manifestation of this binding mechanism (Figure 5E,F). According to this model, the positively charged amino group of G(2′H,3′NH$_3^+$) provides a "binding anchor" that increases the residency time of an early complex in the binding and thus association rate constants.[b] Indeed, the observation of an increase in the association rate constant, relative to that of G, indicates that the −NH$_3^+$ interaction is formed prior to the transition state for complex formation.

As RNAs are replete with negatively charged phosphoryl groups and other hydrogen bond acceptors, the introduction of well-placed −NH$_3^+$ groups or other positively charged moieties may provide a generalizable means for enhancing binding rates. Our data indicate an association rate enhancement effect of at least 50-fold [$\sim 2$ kcal/mol (Table 3)], but given the strength of electrostatic interactions with RNA (e.g., refs 68 and 69), the ability to make multiple interactions with an −NH$_3^+$ group or other moieties (e.g., ref 70), and the fact that our −NH$_3^+$ interaction appears to be fortuitous, considerably larger effects may be possible. Such anchors could even be transient, holding binding groups near their binding sites until rearrangements allow for additional interactions, with subsequent rearrangement to a more stable final bound state that does not contain the −NH$_3^+$ interaction. (In this case, the −NH$_3^+$ group would catalyze formation and release of the ligand.)

We speculate than an anchor mechanism may contribute to the efficacy of ribosome binding aminoglycoside antibiotics. These small molecules have been shown to bind to numerous RNAs, likely at multiple sites, so their efficacy as specific drugs is even more remarkable.[40,41,68,71,72] Perhaps their efficacy is enhanced by fast binding that allows binding to and trapping of a transient ribosomal state. With the renewed interest in drugs for targeting RNAs,[16−18] it is important to continue to develop our fundamental understanding of the kinetics and thermodynamics of RNA/ligand interactions.

## ASSOCIATED CONTENT

**Ⓢ Supporting Information**

The Supporting Information is available free of charge on the ACS Publications website at DOI: 10.1021/acs.biochem.9b00231.

> pH dependence of binding of G and G analogues to the ribozyme (PDF)

## AUTHOR INFORMATION

**Corresponding Author**

*E-mail: herschla@stanford.edu.

**ORCID** Ⓞ

Daniel Herschlag: 0000-0002-4685-1973

## ADDITIONAL NOTES

[a]The pulse−chase assay provides valuable information for binding of G(2′H,3′NH$_3^+$), but the kinetic parameters obtained are limits and were obtained indirectly. To obtain values for these rate constants and to probe complex binding mechanisms that may involve more than two observable states (e.g., Figure 5), 2-aminopurine riboside and its corresponding derivatives with −NH$_3^+$ and/or −H substituents might be used with mutant ribozymes to follow binding in real time via 2-aminopurine fluorescence (e.g., refs 73 and 74).

[b]The effect of the −NH$_3^+$ substituent on the binding of G to the ribozyme presumably arises from electrostatic interactions (see Figures S1−S6). However, additional contributors, including differences in hydrogen bonding, steric accessibility, sugar pucker, and inductive effects among the G analogues, are possible and remain to be tested (e.g., ref 75).

## REFERENCES

(1) Tucker, B. J., and Breaker, R. R. (2005) Riboswitches as versatile gene control elements. *Curr. Opin. Struct. Biol.* 15, 342−348.

(2) Jones, C. P., and Ferre-D'Amare, A. R. (2017) Long-Range Interactions in Riboswitch Control of Gene Expression. *Annu. Rev. Biophys.* 46, 455−481.

(3) Furtig, B., Nozinovic, S., Reining, A., and Schwalbe, H. (2015) Multiple conformational states of riboswitches fine-tune gene regulation. *Curr. Opin. Struct. Biol.* 30, 112−124.

(4) Zhou, J., and Rossi, J. (2017) Aptamers as targeted therapeutics: current potential and challenges. *Nat. Rev. Drug Discovery* 16, 440.

(5) Patel, D. J., Suri, A. K., Jiang, F., Jiang, L., Fan, P., Kumar, R. A., and Nonin, S. (1997) Structure, recognition and adaptive binding in RNA aptamer complexes. *J. Mol. Biol.* 272, 645−664.

(6) Bunka, D. H., and Stockley, P. G. (2006) Aptamers come of age - at last. *Nat. Rev. Microbiol.* 4, 588−596.

(7) Sengupta, R. N., Van Schie, S. N., Giambasu, G., Dai, Q., Yesselman, J. D., York, D., Piccirilli, J. A., and Herschlag, D. (2016) An active site rearrangement within the Tetrahymena group I ribozyme releases nonproductive interactions and allows formation of catalytic interactions. *RNA* 22, 32−48.

(8) Hougland, J., Piccirilli, J., Forconi, M., Lee, J., and Herschlag, D. (2006) How the group I intron works: a case study of RNA structure and function. In *RNA World*, 3rd ed., pp 133−205, Cold Spring Harbor Laboratory Press, Plainview, NY.

(9) Higgs, P. G., and Lehman, N. (2015) The RNA World: molecular cooperation at the origins of life. *Nat. Rev. Genet.* 16, 7.

(10) Gilbert, W. (1986) Origin of life: The RNA world. *Nature* 319, 618−618.

(11) Breaker, R. R. (2012) Riboswitches and the RNA world. *Cold Spring Harbor Perspect. Biol.* 4, a003566.

(12) Gleitsman, K. R., Sengupta, R. N., and Herschlag, D. (2017) Slow molecular recognition by RNA. *RNA* 23, 1745−1753.

(13) Sigler, P. B. (1975) *Annu. Rev. Biophys. Bioeng.* 4, 477−527.

(14) Russell, R. (2008) RNA misfolding and the action of chaperones. *Front. Biosci., Landmark Ed.* 13, 1−20.

(15) Herschlag, D. (1995) RNA chaperones and the RNA folding problem. *J. Biol. Chem.* 270, 20871−20874.

(16) Warner, K. D., Hajdin, C. E., and Weeks, K. M. (2018) Principles for targeting RNA with drug-like small molecules. *Nat. Rev. Drug Discovery* 17, 547−558.

(17) Sullenger, B. A., and Nair, S. (2016) From the RNA world to the clinic. *Science 352*, 1417−1420.

(18) Guan, L., and Disney, M. D. (2012) Recent advances in developing small molecules targeting RNA. *ACS Chem. Biol. 7*, 73−86.

(19) Chappell, J., Watters, K. E., Takahashi, M. K., and Lucks, J. B. (2015) A renaissance in RNA synthetic biology: new mechanisms, applications and tools for the future. *Curr. Opin. Chem. Biol. 28*, 47−56.

(20) Zhang, Z., Witham, S., and Alexov, E. (2011) On the role of electrostatics in protein-protein interactions. *Phys. Biol. 8*, 035001.

(21) Sheinerman, F. B., Norel, R., and Honig, B. (2000) Electrostatic aspects of protein-protein interactions. *Curr. Opin. Struct. Biol. 10*, 153−159.

(22) Lo Conte, L., Chothia, C., and Janin, J. (1999) The atomic structure of protein-protein recognition sites. *J. Mol. Biol. 285*, 2177−2198.

(23) Hemsath, L., Dvorsky, R., Fiegen, D., Carlier, M. F., and Ahmadian, M. R. (2005) An electrostatic steering mechanism of Cdc42 recognition by Wiskott-Aldrich syndrome proteins. *Mol. Cell 20*, 313−324.

(24) Barlow, D. J., and Thornton, J. M. (1986) The distribution of charged groups in proteins. *Biopolymers 25*, 1717−1733.

(25) Wallis, R., Moore, G. R., James, R., and Kleanthous, C. (1995) Protein-protein interactions in colicin E9 DNase-immunity protein complexes. 1. Diffusion-controlled association and femtomolar binding for the cognate complex. *Biochemistry 34*, 13743−13750.

(26) Schreiber, G., Haran, G., and Zhou, H. X. (2009) Fundamental aspects of protein-protein association kinetics. *Chem. Rev. 109*, 839−860.

(27) Schreiber, G., and Fersht, A. R. (1996) Rapid, electrostatically assisted association of proteins. *Nat. Struct. Biol. 3*, 427−431.

(28) Radić, Z., Kirchhoff, P. D., Quinn, D. M., McCammon, J. A., and Taylor, P. (1997) Electrostatic influence on the kinetics of ligand binding to acetylcholinesterase: distinctions between active center ligands and fasciculin. *J. Biol. Chem. 272*, 23265−23277.

(29) Polticelli, F., Battistoni, A., O'Neill, P., Rotilio, G., and Desideri, A. (1998) Role of the electrostatic loop charged residues in Cu,Zn superoxide dismutase. *Protein Sci. 7*, 2354−2358.

(30) Lambeth, J. D., Seybert, D. W., and Kamin, H. (1980) Adrenodoxin reductase. adrenodoxin complex. Rapid formation and breakdown of the complex and a slow conformational change in the flavoprotein. *J. Biol. Chem. 255*, 4667−4672.

(31) von Hippel, P. H., and Berg, O. G. (1989) Facilitated target location in biological systems. *J. Biol. Chem. 264*, 675−678.

(32) Halford, S. E. (2009) An end to 40 years of mistakes in DNA-protein association kinetics? *Biochem. Soc. Trans. 37*, 343−348.

(33) Esadze, A., and Stivers, J. T. (2018) Facilitated Diffusion Mechanisms in DNA Base Excision Repair and Transcriptional Activation. *Chem. Rev. 118*, 11298−11323.

(34) Lipfert, J., Doniach, S., Das, R., and Herschlag, D. (2014) Understanding nucleic acid-ion interactions. *Annu. Rev. Biochem. 83*, 813−841.

(35) Draper, D. E., Grilley, D., and Soto, A. M. (2005) Ions and RNA folding. *Annu. Rev. Biophys. Biomol. Struct. 34*, 221−243.

(36) Chu, V. B., Bai, Y., Lipfert, J., Herschlag, D., and Doniach, S. (2008) A repulsive field: advances in the electrostatics of the ion atmosphere. *Curr. Opin. Chem. Biol. 12*, 619−625.

(37) Manning, G. S. (1978) The molecular theory of polyelectrolyte solutions with applications to the electrostatic properties of polynucleotides. *Q. Rev. Biophys. 11*, 179−246.

(38) Draper, D. E. (2008) RNA folding: thermodynamic and molecular descriptions of the roles of ions. *Biophys. J. 95*, 5489−5495.

(39) Zapp, M. L., Stern, S., and Green, M. R. (1993) Small molecules that selectively block RNA binding of HIV-1 Rev protein inhibit Rev function and viral production. *Cell 74*, 969−978.

(40) Walter, F., Vicens, Q., and Westhof, E. (1999) Aminoglycoside-RNA interactions. *Curr. Opin. Chem. Biol. 3*, 694−704.

(41) Vicens, Q., and Westhof, E. (2003) RNA as a drug target: the case of aminoglycosides. *ChemBioChem 4*, 1018−1023.

(42) Rogers, J., Chang, A. H., von Ahsen, U., Schroeder, R., and Davies, J. (1996) Inhibition of the self-cleavage reaction of the human hepatitis delta virus ribozyme by antibiotics. *J. Mol. Biol. 259*, 916−925.

(43) Mikkelsen, N. E., Brannvall, M., Virtanen, A., and Kirsebom, L. A. (1999) Inhibition of RNase P RNA cleavage by aminoglycosides. *Proc. Natl. Acad. Sci. U. S. A. 96*, 6155−6160.

(44) Lando, D., Cousin, M. A., and Privat de Garilhe, M. (1973) Misreading, a fundamental aspect of the mechanism of action of several aminoglycosides. *Biochemistry 12*, 4528−4533.

(45) Herschlag, D., Khosla, M., Tsuchihashi, Z., and Karpel, R. L. (1994) An RNA chaperone activity of non-specific RNA binding proteins in hammerhead ribozyme catalysis. *EMBO J. 13*, 2913−2924.

(46) Bayer, T. S., Booth, L. N., Knudsen, S. M., and Ellington, A. D. (2005) Arginine-rich motifs present multiple interfaces for specific binding by RNA. *RNA 11*, 1848−1857.

(47) Allers, J., and Shamoo, Y. (2001) Structure-based analysis of protein-RNA interactions using the program ENTANGLE. *J. Mol. Biol. 311*, 75−86.

(48) Korennykh, A. V., Piccirilli, J. A., and Correll, C. C. (2006) The electrostatic character of the ribosomal surface enables extraordinarily rapid target location by ribotoxins. *Nat. Struct. Mol. Biol. 13*, 436−443.

(49) Zaug, A. J., Grosshans, C. A., and Cech, T. R. (1988) Sequence-specific endoribonuclease activity of the Tetrahymena ribozyme: enhanced cleavage of certain oligonucleotide substrates that form mismatched ribozyme-substrate complexes. *Biochemistry 27*, 8924−8931.

(50) Kladwang, W., Hum, J., and Das, R. (2012) Ultraviolet Shadowing of RNA Can Cause Significant Chemical Damage in Seconds. *Sci. Rep. 2*, 517.

(51) Herschlag, D., Eckstein, F., and Cech, T. R. (1993) Contributions of 2′-hydroxyl groups of the RNA substrate to binding and catalysis by the Tetrahymena ribozyme. An energetic picture of an active site composed of RNA. *Biochemistry 32*, 8299−8311.

(52) Karbstein, K., Carroll, K. S., and Herschlag, D. (2002) Probing the Tetrahymena group I ribozyme reaction in both directions. *Biochemistry 41*, 11171−11183.

(53) McConnell, T. S., Cech, T. R., and Herschlag, D. (1993) Guanosine binding to the Tetrahymena ribozyme: thermodynamic coupling with oligonucleotide binding. *Proc. Natl. Acad. Sci. U. S. A. 90*, 8362−8366.

(54) Knitt, D. S., and Herschlag, D. (1996) pH dependencies of the Tetrahymena ribozyme reveal an unconventional origin of an apparent pKa. *Biochemistry 35*, 1560−1570.

(55) Herschlag, D., and Khosla, M. (1994) Comparison of pH dependencies of the Tetrahymena ribozyme reactions with RNA 2′-substituted and phosphorothioate substrates reveals a rate-limiting conformational step. *Biochemistry 33*, 5291−5297.

(56) Shan, S. O., and Herschlag, D. (1999) Probing the role of metal ions in RNA catalysis: kinetic and thermodynamic characterization of a metal ion interaction with the 2′-moiety of the guanosine nucleophile in the Tetrahymena group I ribozyme. *Biochemistry 38*, 10958−10975.

(57) Stahley, M. R., and Strobel, S. A. (2005) Structural evidence for a two-metal-ion mechanism of group I intron splicing. *Science 309*, 1587−1590.

(58) Lipchock, S. V., and Strobel, S. A. (2008) A relaxed active site after exon ligation by the group I intron. *Proc. Natl. Acad. Sci. U. S. A. 105*, 5699−5704.

(59) Shan, S. O., Narlikar, G. J., and Herschlag, D. (1999) Protonated 2′-aminoguanosine as a probe of the electrostatic environment of the active site of the Tetrahymena group I ribozyme. *Biochemistry 38*, 10976−10988.

(60) Hougland, J. L., Sengupta, R. N., Dai, Q., Deb, S. K., and Piccirilli, J. A. (2008) The 2′-hydroxyl group of the guanosine nucleophile donates a functionally important hydrogen bond in the tetrahymena ribozyme reaction. *Biochemistry 47*, 7684−7694.

(61) Karbstein, K., and Herschlag, D. (2003) Extraordinarily slow binding of guanosine to the Tetrahymena group I ribozyme:

implications for RNA preorganization and function. *Proc. Natl. Acad. Sci. U. S. A. 100*, 2300−2305.

(62) Jucker, F. M., Phillips, R. M., McCallum, S. A., and Pardi, A. (2003) Role of a heterogeneous free state in the formation of a specific RNA-theophylline complex. *Biochemistry 42*, 2560−2567.

(63) Flinders, J., DeFina, S. C., Brackett, D. M., Baugh, C., Wilson, C., and Dieckmann, T. (2004) Recognition of planar and nonplanar ligands in the malachite green-RNA aptamer complex. *ChemBioChem 5*, 62−72.

(64) Duchardt-Ferner, E., Weigand, J. E., Ohlenschlager, O., Schmidtke, S. R., Suess, B., and Wohnert, J. (2010) Highly modular structure and ligand binding by conformational capture in a minimalistic riboswitch. *Angew. Chem., Int. Ed. 49*, 6216−6219.

(65) Woodside, M. T., Anthony, P. C., Behnke-Parks, W. M., Larizadeh, K., Herschlag, D., and Block, S. M. (2006) Direct measurement of the full, sequence-dependent folding landscape of a nucleic acid. *Science 314*, 1001−1004.

(66) Porschke, D. (1977) Elementary steps of base recognition and helix-coil transitions in nucleic acids. *Mol. Biol., Biochem. Biophys. 24*, 191−218.

(67) Bloomfield, V., Crothers, D., and Tinoco, I. (2000) *Nucleic acids: structure, properties, and functions*, University Science Books, Sausalito, CA.

(68) Stage, T. K., Hertel, K. J., and Uhlenbeck, O. C. (1995) Inhibition of the hammerhead ribozyme by neomycin. *RNA 1*, 95−101.

(69) Clouet-D'Orval, B., Stage, T. K., and Uhlenbeck, O. C. (1995) Neomycin inhibition of the hammerhead ribozyme involves ionic interactions. *Biochemistry 34*, 11186−11190.

(70) François, B., Russell, R. J., Murray, J. B., Aboul-Ela, F., Masquida, B., Vicens, Q., and Westhof, E. (2005) Crystal structures of complexes between aminoglycosides and decoding A site oligonucleotides: role of the number of rings and positive charges in the specific binding leading to miscoding. *Nucleic Acids Res. 33*, 5677−5690.

(71) Wang, H., and Tor, Y. (1997) Electrostatic Interactions in RNA Aminoglycosides Binding. *J. Am. Chem. Soc. 119*, 8734−8735.

(72) Trylska, J., and Kulik, M. (2016) Interactions of aminoglycoside antibiotics with rRNA. *Biochem. Soc. Trans. 44*, 987−993.

(73) Michel, F., Hanna, M., Green, R., Bartel, D. P., and Szostak, J. W. (1989) The guanosine binding site of the Tetrahymena ribozyme. *Nature 342*, 391−395.

(74) Gilbert, S. D., Stoddard, C. D., Wise, S. J., and Batey, R. T. (2006) Thermodynamic and kinetic characterization of ligand binding to the purine riboswitch aptamer domain. *J. Mol. Biol. 359*, 754−768.

(75) Gordon, P. M., Fong, R., Deb, S. K., Li, N. S., Schwans, J. P., Ye, J. D., and Piccirilli, J. A. (2004) New strategies for exploring RNA's 2′-OH expose the importance of solvent during group II intron catalysis. *Chem. Biol. 11*, 237−246.